Investigation of Copper Halide: Hydrothermal Syntheses and Characterization of $CuBr_2(C_{12}H_8N_2)$ and $Cu_3Br_3(C_{12}H_8N_2)_2$

ZHAO, Xiao-Li[a](赵小莉) XU, Ji-Qing*,[a,b](徐吉庆) ZHANG, Li-Juan[a](张丽娟)
YU, Jie-Hui[a](于杰辉) ZENG, Qing-Xin[a](曾庆新) CUI, Xiao-Bing[a](崔小兵)
WANG, Tie-Gang[a](王铁刚) WANG, Tian-Wei[b](王天维)

[a] *College of Chemistry and State Key Laboratory of Inorganic Synthesis and Preparative Chemistry, Jilin University, Changchun, Jilin 130023, China*

[b] *State Key Laboratory of Coordination Chemistry, Nanjing University, Nanjing, Jiangsu 210093, China*

The reaction of $CuBr_2$ with 1,10-phen-H_2O (1,10-phen = 1,10-phenanthroline) gave two compounds: $CuBr_2(C_{12}H_8N_2)$ and $Cu_3Br_3(C_{12}H_8N_2)_2$. Their structures have been characterized by single-crystal X-ray diffraction analysis, elemental analyses, thermogravimetric analyses (TGA) and measurement of variable temperature magnetic susceptibility. Crystal data for $CuBr_2(C_{12}H_8N_2)$: monoclinic, space group $P2_1/n$, $a = 0.9977(3)$ nm, $b = 0.65138(14)$ nm, $c = 1.8207(4)$ nm, $\beta = 91.624(18)°$, $V = 1.1828(5)$ nm^3, $Z = 2$. Crystal data for $Cu_3Br_3(C_{12}H_8N_2)_2$: monoclinic, space group $C2/c$, $a = 1.00167(11)$ nm, $b = 1.4523(4)$ nm, $c = 1.6295(3)$ nm, $\beta = 94.386(14)°$, $V = 2.3635(8)$ nm^3, $Z = 3$.

Keywords copper halide, crystal structure, hydrothermal synthesis

Introduction

The construction of inorganic-organic compound arrays based on covalent interactions[1] or hydrogen bonding[2] is a rapidly developing area of research that has implication for the rational design of functional materials. Supramolecular materials with a variety of architectures have been reported including adamantoid,[3-5] octahedral,[6] ladder,[7] honeycomb,[8] brick wall,[9] *etc*. The reaction of copper halides with organic ligands has been studied extensively.[10] All these have provoked our interest in the hydrothermal syntheses of copper halide with different framework structures that are templated by bulky organic ligands. One aspect of our investigation has been focused on the reaction of $CuBr_2$-1,10-phen-H_2O system under mild hydrothermal conditions. Here the syntheses and characterizations of supramolecular network structure $CuBr_2(C_{12}H_8N_2)$ (**1**) and molecular cluster $Cu_3Br_3(C_{12}H_8N_2)_2$ (**2**) are reported.

Experimental

Syntheses

The starting material in all syntheses are of reagent grade from commercial sources without further purification.

Synthesis of compound **1**

To 20 mL of H_2O was added $CuBr_2$(0.4 g, 1.8 mmol), CuCl (0.3 g, 1.0 mmol) and 1,10-phen (0.6 g, 1.0 mmol). The reaction mixture was sealed in a 30-mL Teflon-lined stainless steel vessel and heated under autogenous pressure at 160 ℃ for 5 d. Dark-green columnar crystals were obtained in a total yield of approximately 75% [based on Cu(II)].

Synthesis of compound **2**

To 20 mL of H_2O was added $CuBr_2$(0.4 g, 1.8 mmol), C_6H_4-1,4-$(CO_2H)_2$(0.33 g, 2.00 mmol), KOH (0.5 g, 9.0 mmol), 1,10-phen (0.4 g, 2.0 mmol) and $FeSO_4$ (0.57 g, 2.00 mmol). The reaction mixture was sealed in a 30-mL Teflon-lined stainless steel vessel and heated under autogenous pressure at 160 ℃ for 5 d. Dark-red columnar crystals were obtained in a total yield of approximately 60% [based on Cu(II)].

Elemental analyses

Elemental analyses for C, H and N were performed on a

* E-mail: xjq@mail.jlu.edu.cn

Received December 10, 2001; revised May 13, 2002; accepted November 2, 2002.

Project supported by the National Natural Science Foundation of China (No. 20271021) and the Research Funds for the Doctoral Program of High Education (No. 1999018310).

Perkin-Elmer 2400LS II element analyzer. Inductively coupled plasma (ICP) analysis for Cu was conducted on a Jarrzall-ash 800 Mark-II ICP instrument. Anal. calcd for **1**: C 35.76, H 1.98, N 6.94, Cu 15.75; found C 35.72, H 1.77, N 6.85, Cu 15.94. Anal. calcd for **2**: C 36.46, H 2.02, N 7.09, Cu 24.11; found C 36.12, H 2.15, N 7.18, Cu 24.02.

TGA analyses

A Perkin-Elmer TGA 7 thermogravimetric analyzer (TGA) was used to obtain TGA curves in air with a rate of temperature increase of 20 ℃/min and at temperature range of room temperature to 780 ℃.

Measurement of magnetic property

Variable temperature magnetic susceptibility of compound **1** was measured on a CAHN 2000 Faraday Magnetic Balance at temperature range of 75—300 K.

Determination of crystal structure

Crystals of **1** and **2** suitable for single-crystal X-ray diffraction analysis with size 0.32 mm × 0.25 mm × 0.16 mm and 0.46 mm × 0.32 mm × 0.25 mm were selected, respectively. Structural analyses were performed on a Siemens SMART CCD diffractometer using graphite-monochromated Mo Kα radiation ($\lambda = 0.071073$ nm). The data were collected at temperature (20 ± 2) ℃. Data processing was accomplished with the SAINT processing program.[11] Direct methods were used to solve structure using the SHELXTL crystallographic software package.[12]

Results and discussion

Syntheses

In the synthesis of compound **1**, our original target is to synthesize mixed valance copper halide, but only compound **1** with Cu(II) was obtained.

In preparing compound **2**, it was expected to synthesize mixed metal cluster with Cu and Fe, but only produced compound **2** with Cu(I).

Compound **2** was synthesized under alkaline condition. Relevant reactions and their standard oxidation-reduction potentials under alkaline condition are given as follows:

$$Fe(OH)_3 + e \leftrightarrow Fe(OH)_2 + OH^- \quad -0.56\ V \qquad (1)$$

$$2Cu(OH)_2 + 2e \leftrightarrow Cu_2O + 2OH^- + H_2O \quad -0.08\ V \qquad (2)$$

From above it can be concluded that the following reaction [Eq. (3)] may happen to produce Cu^+ ions under alkaline condition:

$$Fe^{2+} + Cu^{2+} \longrightarrow Fe^{3+} + Cu^+ \qquad (3)$$

The formation process of compound **2** may be written as Eq. (4):

$$CuBr + Br^- \rightarrow CuBr_2^- \qquad (4)$$

$$2\ CuBr + 2\ phen \longrightarrow phenCu\begin{matrix}Br\\ \diagup\ \diagdown\\ Br\end{matrix}phenCu \qquad (5)$$

$$phenCu\begin{matrix}Br\\ \diagup\ \diagdown\\ Br\end{matrix}phenCu + CuBr_2^- \longrightarrow Cu_3Br_3phen_2 + Br^- \qquad (6)$$

Structure description

Crystallographic data and refinement details of compounds **1** and **2** are summarized in Table 1. Selected bonds lengths and angles are shown in Tables 2 and 3 for compounds **1** and **2**, respectively. Atomic coordinates and equivalent isotropic displacement parameters are listed in Tables 4 and 5, respectively.

Table 1 Crystal data and structure refinement for $CuBr_2(C_{12}H_8N_2)$ (**1**) and $Cu_3Br_3(C_{12}H_8N_2)_2$ (**2**)

Molecular formula	$CuC_{12}H_8N_2Br_2$	$Cu_3C_{24}H_{16}N_4Br_3$
crystal system	Monoclinic	Monoclinic
space group	$P2_1/n$	$C2/c$
a (nm)	0.9977(3)	1.00167(11)
b (nm)	0.65138(14)	1.4523(4)
c (nm)	1.8207(4)	1.6295(3)
β (°)	91.624(18)	94.386(14)
V (nm^3)	1.1828(5)	2.3635(8)
D_c (g/cm^3)	1.133	1.667
Z	2	3
θ range (°)	2.24 to 23.27	2.47 to 25.01
T (K)	293(2)	293(2)
Goodness-of-fit on F^2	0.965	0.864

Continued

Absorption coefficient	4.288 mm^{-1}	5.827 mm^{-1}
$F(000)$	386	2280
Completeness	74.0% ($\theta = 23.27$)	99.9% ($\theta = 25.01$)
Refinement method	Full-matrix least-squares on F^2	Full-matrix least-squares on F^2
Data/restraints/parameters	1260/12/154	2087/0/192
Reflections collected/unique	1842/1260 [$R_{int} = 0.0420$]	2785/2087 [$R_{int} = 0.0447$]
Final R indices [$I > 2\sigma(I)$]	$R_1 = 0.0472$, $wR_2 = 0.1150$	$R_1 = 0.0388$, $wR_2 = 0.0841$
R indices (all data)	$R_1 = 0.0735$, $wR_2 = 0.1287$	$R_1 = 0.0720$, $wR_2 = 0.0901$
Largest diff. peak and hole (e/nm^3)	1.222×10^{-3} and -8.94×10^{-4}	4.70×10^{-4} and -4.74×10^{-4}

Table 2 Selected bonds lengths (nm) and angles (°) for $CuBr_2(C_{12}H_8N_2)$ (**1**)

Cu(1)—N(2)	0.2036(8)
Cu(1)—N(1)	0.2038(10)
Cu(1)—Br(2)	0.23675(15)
Cu(1)—Br(1)	0.23978(19)
N(2)-Cu(1)-N(1)	81.9(4)
N(2)-Cu(1)-Br(2)	175.1(3)
N(1)-Cu(1)-Br(2)	93.9(2)
N(2)-Cu(1)-Br(1)	92.6(3)
N(1)-Cu(1)-Br(1)	173.4(2)
Br(2)-Cu(1)-Br(1)	91.82(6)
C(12)-N(1)-Cu(1)	110.7(8)
C(1)-N(1)-Cu(1)	131.1(7)
C(10)-N(2)-Cu(1)	130.5(8)
C(11)-N(2)-Cu(1)	110.5(8)

Table 3 Selected bond lengths (nm) and angles (°) for $Cu_3Br_3(C_{12}H_8N_2)_2$ (**2**)[a]

Br(1)—Cu(1)	0.22899(18)
Br(1)—Cu(2)	0.24164(12)
Br(1)—Cu(2A)	0.26461(12)
Br(2)—Cu'	0.22179(19)
Br(2)—Cu(1)	0.22179(19)
Cu(2)—N(1)	0.2050(5)
Cu(2)—N(2)	0.2060(5)
Cu(1)-Br(1)-Cu(2)	66.34(5)
Cu(1)-Br(1)-Cu(2A)	64.94(6)
Cu(2)-Br(1)-Cu(2A)	79.33(4)
Cu'(1)-Br(2)-Cu(1)	28.33(10)
N(1)-Cu(2)-N(2)	82.47(19)
N(1)-Cu(2)-Br(1)	139.81(16)
N(2)-Cu(2)-Br(1)	111.83(14)
N(1)-Cu(2)-Br(1A)	104.67(15)
N(2)-Cu(2)-Br(1A)	119.56(15)
Br(1)-Cu(2)-Br(1A)	100.09(4)
Br(2)-Cu(1)-Br(1)	156.45(9)
Br(2)-Cu(1)-Cu(2)	135.90(9)
C(10)-N(1)-Cu(2)	131.1(4)
C(11)-N(1)-Cu(2)	110.6(4)
C(1)-N(2)-Cu(2)	131.0(4)
C(12)-N(2)-Cu(2)	111.0(4)

[a] symmetry code: A $-x$, y, $-z+1/2$.

Table 4 Atomic coordinates ($\times 10^4$) and equivalent isotropic displacement parameters ($nm^2 \times 10^5$) for $CuBr_2(C_{10}H_8N_2)$ (**1**)

Atom	x	y	z	U_{eq}[a]
Cu(1)	6407(1)	2237(2)	7618(1)	32(1)
Br(1)	8644(1)	2266(2)	7171(1)	43(1)
Br(2)	5469(1)	2125(2)	6410(1)	53(1)
N(1)	4591(11)	404(12)	8100(4)	30(2)
N(2)	7069(10)	209(12)	8687(4)	27(2)
C(1)	3314(14)	534(18)	7794(6)	41(3)
C(2)	2260(20)	690(19)	8210(7)	65(5)
C(3)	2387(17)	765(17)	8958(7)	56(4)
C(4)	3551(14)	618(15)	9301(6)	35(3)
C(5)	3848(17)	637(14)	10090(6)	52(5)
C(6)	5104(15)	549(14)	10375(5)	31(3)
C(7)	6233(15)	376(13)	9923(5)	34(4)
C(8)	7530(15)	276(15)	10197(5)	36(3)
C(9)	8590(15)	137(15)	9723(5)	45(4)
C(10)	8271(14)	130(15)	8964(5)	38(3)
C(11)	5985(13)	360(13)	9154(5)	24(3)
C(12)	4747(13)	432(14)	8852(5)	27(3)

[a] U_{eq} is defined as one third of the trace of the orthogonalized U_{ij} tensor.

Table 5 Atomic coordinates ($\times 10^4$) and equivalent isotropic displacement parameters ($nm^2 \times 10^5$) for $Cu_3Br_3(C_{12}H_8N_2)$ (**2**)

Atom	x	y	z	U_{eq}[a]
Br(1)	1843(1)	2056(1)	2966(1)	43(1)
Br(2)	0	4784(1)	2500	60(1)
Cu(1)	521(2)	3303(1)	2617(1)	63(1)
Cu(2)	655(1)	1932(1)	1623(1)	64(1)
N(1)	1242(5)	792(3)	991(3)	39(1)
N(2)	627(5)	2525(4)	480(3)	39(1)
C(1)	328(7)	3361(5)	235(4)	45(2)
C(2)	313(7)	3650(5)	-589(4)	50(2)
C(3)	651(7)	3034(5)	-1168(4)	0(2)
C(4)	994(6)	2121(4)	-934(4)	40(2)
C(5)	1377(7)	1428(5)	-1494(3)	50(2)
C(6)	1718(7)	571(5)	-1234(4)	48(2)
C(7)	1696(6)	326(4)	-386(3)	38(2)
C(8)	2037(7)	-551(5)	-88(4)	4(2)
C(9)	2014(7)	-735(5)	731(4)	52(2)
C(10)	1602(7)	-24(5)	1248(4)	48(2)
C(11)	1314(6)	987(4)	175(3)	33(1)
C(12)	959(6)	1896(4)	-92(3)	31(1)

[a] U_{eq} is defined as one third of the trace of the orthogonalized U_{ij} tensor.

Compound **1** Structure analysis of $CuBr_2(C_{10}H_8N_2)$ shows that the crystals of **1** are constructed with discrete units $CuBr_2(C_{10}H_8N_2)$. In the discrete unit (Fig. 1), copper atom is in a quasi-planar tetra-coordination environment formed from two nitrogen atoms of 1,10-phen ligand (Cu—N 0.2036(8) nm and 0.2038(10) nm, respectively) and two bromine atoms (Cu—Br 0.23675(15) nm and 0.23978(19) nm, respectively). The deviation of Cu from the mean quasi-planar is 0.00112 nm. The discrete units are then joined together to form a 2-D layer via H-bonding along *a*-axis as confirmed from the distances of H···Br and C—H···Br and the angles of C—H···Br[13] as shown in Table 6. The dihedrals between the unit Cu(1) and unit Cu(1A) or unit Cu(1B) both are 3.6°, and the unit Cu(1A) and unit Cu(1B) are parallel. The layers are then linked together via π-π interaction of the interpenetration of phen rings along *b*-axis and the semi-coordinate Cu—Br bonds to form a three-dimensional supramolecular network as shown in Figs. 2 and 3. Cu(1L)—Br(1C) and Cu(1K)—Br(1C) bond distances, and the distance between interdigital and parallel phen rings are 0.3261 nm, 0.3299 nm and 0.3257 nm, respectively. All these indicate the existence of semicoordinate bonds[10] and π-π interactions.[14]

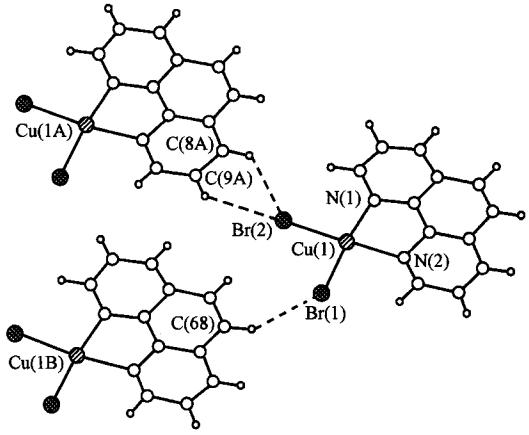

Fig. 1 Molecular structure of $CuBr_2(C_{12}H_8N_2)$ (**1**) and representation of hydrogen-bonding.

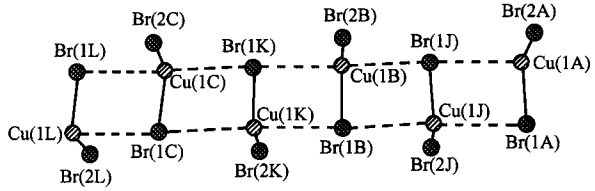

Fig. 2 Linkage of Cu—Br semicoordinating bonding between $CuBr_2(C_{12}H_8N_2)$ (**1**) molecules.

Table 6 Bond lengths (nm) and angles (°) of hydrogen bonds of $CuBr_2(C_{12}H_8N_2)$ (**1**)

Hydrogen bond	H···X	Y—H···X	Angle
C(6B)—H···Br(1A)	0.2871	0.3619	138.3°
C(8C)—H···Br(2A)	0.3042	0.3642	123.8°
C(9C)—H···Br(2A)	0.2948	0.3585	126.9°

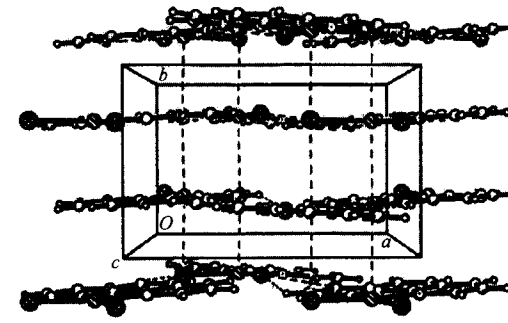

Fig. 3 View of the 3-D supramolecular structure linked by Cu—Br semicoordinating bonds and π-π interactions between phen rings.

Compound **2** The molecular structure of $Cu_3Br_3(C_{12}H_8N_2)_2$ is displayed in Fig. 4. It is a non-centro symmetric trinuclear cluster: Cu(1), Cu(2), Cu(2A). There exists a 2-fold axis through Br(2) atom along the line of *b*. Cu(1) is a disordered atom. Cu(1) and Cu′ each has occupancy 0.5. The two copper atoms Cu(1) and Cu(2) occur in a 2- and 4-coordinate sited site, respectively. Cu(2) atom at the tetrahedral center is coordinated by two bridging bromine atoms and two nitrogen atoms from the 1,10-phen molecule with Cu—Br bond length range from 0.24164(12) nm [Br(1)—Cu(2)] to 0.26461(12) nm [Cu(2)—Br(1A)] and Cu—N bond length range from 0.2060(5) nm [Cu(2)—N(2)] to 0.2050(5) nm [Cu(2)—N(1)]. Cu(1) is coordinated by one bridging and one terminal bromine atom with the terminal Cu(1)—Br(2) distance of 0.22179(19) nm and the longer bridging Cu(1)—Br(1) distance of 0.22899(18) nm. The dihedral of planes Cu(2)-Br(1)-Cu(2A) and Cu(2)-Br(1A)-Cu(2A) is 169.4°. This indicates that the four atoms Cu(2), Br(1), Cu(2A) and Br(1A) are not strictly in the same plane. The phen ring coordinated to Cu(2) is not perpendicular to planes Cu(2)-Br(1)-Cu(2A) and Cu(2)-Br(1A)-Cu(2A), but have dihedrals 69.1° and 79.1°, respectively. There is a dihedral of 31.8° between the two phen rings coordinated to Cu(2) and Cu(2A) respectively.

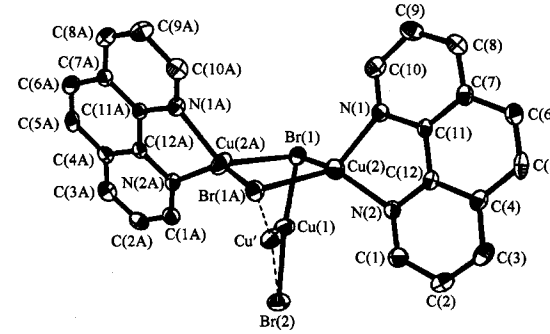

Fig. 4 Molecular structure of $Cu_3Br_3(C_{12}H_8N_2)_2$(**2**).

TGA *analyses*

The TGA curves of compounds **1** and **2** are shown in Fig. 5. It can be seen that both curves are lack of obvious inflection point, which are in agreement with the previously ob-

tained TGA analyses for other copper halide clusters.[15]

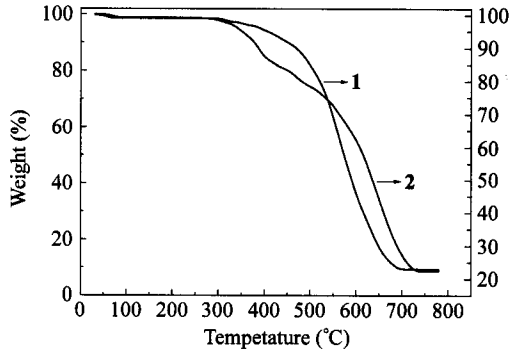

Fig. 5 TGA curves of compound $CuBr_2(C_{12}H_8N_2)$ (**1**) and $Cu_3Br_3(C_{12}H_8N_2)_2$ (**2**).

Both of the compounds are stable before 310 ℃. As for compound **1**, the weight loss is 91.3% during 310—740.86 ℃, which can be attributed to the dissociation and oxidation decomposition of 1,10-phen (calculated value is 44.6% when completely losing 1,10-phen from **1**) and vaporization of a part of copper halide ($CuBr_2$, m.p. 498 ℃, b.p. 900 ℃).

For compound **2**, the weight loss is 74.62% during 310—720.95 ℃, which can be attributed to the dissociation and decomposition of 1,10-phen (calculated value is 45.57%) and the vaporization of a part of copper halide (CuBr, m.p. 492 ℃, b.p. 1345 ℃).

Magnetic property

Fig. 6 gives the curves of molar susceptibility χ_m and its reciprocal χ_m^{-1} vs. T for **1** respectively. Curie constant C = 0.37 emu·K·mol and Weiss constant θ = − 17.87 K were obtained based on Curie-Weiss law $\chi_m = C/(T-\theta)$. The result above-mentioned shows that there exists weak antiferromagnetic interaction between Cu(II) ions for compound **1**, and the observed magnetic exchange interaction probably conducts through Cu···Br···Cu semicoordinate bonds.

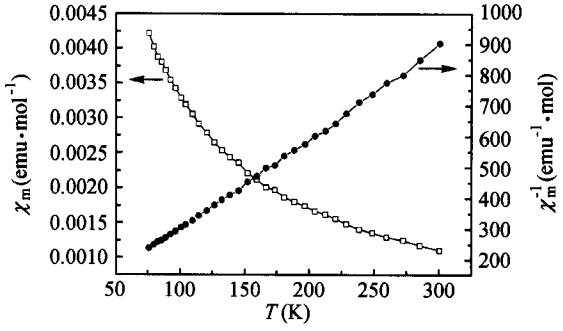

Fig. 6 Plots of χ_m vs. T and χ_m^{-1} vs. T for $CuBr_2(C_{12}H_8N_2)$.

References

1 (a) Robson, R.; Abrahams, B. F.; Batten, S. R.; Gable, R. W.; Hoskins, B. F.; Liu, J. *Supramolecular Architecture*, American Chemical Socity, Washington D. C., **1992**, Chapter 19.
(b) Fujita, M.; Kwon, Y. J.; Washizu, S.; Ogura, K. *J. Am. Chem. Soc.* **1994**, *116*, 1151.

2 (a) Desiraju, G. R. *Crystal Engineering: The Design of Organic Solids*, Amsterdam, Elsevier, **1989**.
(b) Desiraju, G. R. *Angew. Chem., Int. Ed. Engl.* **1995**, *35*, 2311.

3 (a) MacGillvary, L. R.; Subramanian, S.; Zaworotko, M. J. *J. Chem. Soc., Chem. Commun.* **1994**, 1325.
(b) Zaworotko, M. *J. Chem. Soc. Rev.* **1994**, 283.

4 Blake, A. J.; Champness, N. R.; Chung, S. M.; Li, W.-S.; Schröder, M. *Chem. Commun.* **1997**, 1005 and unpublished results.

5 Carlucci, L.; Ciani, G.; Proserpio, D. M.; Sironi, A. *J. Chem. Soc., Chem. Commun.* **1994**, 275.

6 (a) Subramanian, S.; Zaworotko, M. J. *Angew. Chem.* **1995**, *107*, 2295.
(b) Subramanian, S.; Zaworotko, M. J. *Angew. Chem., Int. Ed. Engl.* **1995**, *34*, 2127.

7 (a) Loser, P.; Zaworotko, M. J. *Angew. Chem.* **1996**, *108*, 2957.
(b) Loser, P.; Zaworotko, M. J. *Angew. Chem., Int. Ed. Engl.* **1996**, *35*, 2779.

8 Gardner, G. B.; Venkataramanm, D.; Moore, J. S.; Lee, S. *Nature* **1995**, *374*, 792.

9 Fujita, M.; Kwon, Y. J.; Sasaki, O.; Yamaguchi, K.; Ogura, K. *J. Am. Chem. Soc.* **1995**, *117*, 7287.

10 (a) Hammond, R. P.; Cavaluzzi, M.; Haushalter, R. C.; Zubieta, J. A. *Inorg. Chem.* **1999**, *38*, 1288.
(b) Wei, M.; Willet, R. D. *Inorg. Chem.* **1996**, *35*, 6381.
(c) Chen, X.; Long, G.; Willet, R. D.; Haws, T.; Molnar, S.; Brewer, K. *Acta Crystallogr.* **1996**, *C52*, 1924.
(d) Scott, B.; Willet, R. D.; Saccani, A.; Sandrelint, F.; Ramakrishna, B. L. *Inorg. Chim. Acta* **1996**, *35*, 5300.
(e) Chen, X.; Willet, R. D.; Haws, T.; Molnar, S.; Brewer, K. J. *J. Chem. Crystallogr.* **1996**, *26*, 261.
(f) Pon, G.; Willet, R. D. *Acta Crystallogr.* **1996**, *C52*, 1122.

11 SMART and SAINT (software packages), Siemens Analytical X-ray Instruments, Inc., Madison, WI, **1996**.

12 *SHELXTL*, version 5.1, Siemens, Industrial Automation, Inc., **1997**.

13 Bondi, A. *J. Phys. Chem.* **1964**, *68*, 441.

14 Withersby, M. A.; Blake, A. J.; Champness, N. R.; Hubberstey, P.; Li, W. S.; Schröder, M. *Angew. Chem., Int. Ed. Engl.* **1997**, *36*, 21, 2327.

15 Song, Y. J. *Ph. D. Thesis*, Jilin University, Changchun, **2000** (in Chinese).

(E0112104 ZHAO, X. J.; ZHENG, G. C.)